# Empowering UAV-Based Airborne Computing Platform With SDR: Building an LTE Base Station for Enhanced Aerial Connectivity

Jinran Zhang, *Member, IEEE*, Kejie Lu, *Senior Member, IEEE*, Yan Wan, *Senior Member, IEEE*, Junfei Xie, *Senior Member, IEEE*, and Shengli Fu, *Senior Member, IEEE*

***Abstract*—In recent years, unmanned aerial vehicles (UAVs) have emerged as a transformative technology that can revolutionize various industries and enable a wide range of versatile aerial applications. To facilitate future generations of computing-intensive applications, we have developed a UAV-based airborne computing platform. However, the existing system only supports Wi-Fi connectivity. Recognizing the critical role of Long-Term Evolution (LTE) in providing robust and reliable wireless communication, as well as its compatibility with current and future cellular systems, we present an improved airborne computing platform that combines UAV technology with software-defined radio (SDR). SDR is programmable and can be dynamically configured to enable different wireless communication technologies. Specifically, by using an appropriate SDR module and open-source software, we enhanced the connectivity of our platform by setting it as an LTE base station, thus enabling seamless communication between UAVs and LTE-enabled ground devices. In this paper, we describe the detailed design and implementation of our UAV-based airborne computing platform, emphasizing the integration of SDR technology to build an LTE base station. We also conduct extensive experiments to evaluate the performance of our platform in both indoor and outdoor scenarios, focusing on latency, throughput, signal-to-noise ratio, and resource consumption. Our findings highlight the impact of the computing platform on system performance and emphasize the importance of optimizing software components for specific hardware configurations. Despite the challenges, our results demonstrate the feasibility and potential of SDR-enabled UAV platforms for enhanced aerial connectivity. This work opens up new possibilities for UAV applications, such as edge computing, real-time object detection, remote sensing, and disaster management, all facilitated by the robust and reliable LTE connectivity provided by our UAV-based LTE base station.**

***Index Terms*—Airborne computing platform, communication performance, and resource consumption, long-term evolution (LTE), software-defined radio (SDR), unmanned aerial vehicle (UAV).**

Manuscript received 16 July 2023; revised 28 March 2024; accepted 30 April 2024. Date of publication 12 June 2024; date of current version 17 October 2024. This work was supported in part by the National Science Foundation under Grant CAREER-1714519, Grant CAREER-2048266, and Grant CCRI-2235157/2235158/2235159/2235160. The review of this article was coordinated by Prof. Jun Zheng. *(Corresponding author: Jinran Zhang.)*

Jinran Zhang and Shengli Fu are with the Department of Electrical Engineering, University of North Texas, Denton, TX 76205 USA (e-mail: JinranZhang@my.unt.edu).

Kejie Lu is with the Department of Computer Science and Engineering, University of Puerto Rico at Mayagüez, Mayagüez 00680, Puerto Rico.

Yan Wan is with the Department of Electrical Engineering, University of Texas at Arlington, Arlington, TX 76019 USA.

Junfei Xie is with the Department of Electrical and Computer Engineering, San Diego State University, San Diego, CA 92182 USA.

Digital Object Identifier 10.1109/TVT.2024.3406339

## I. Introduction

In RECENT years, unmanned aerial vehicles (UAVs) have gained significant attractions due to their diverse applications. These applications extend beyond traditional uses in military operations to include areas such as environmental monitoring, disaster management, agricultural surveying, infrastructure inspection, delivery services, and even entertainment in the form of drone light shows. Additionally, UAVs are increasingly used in advanced technological fields, including wireless communications, navigation, distributed computing, and the Internet of Things (IoT) [1]. These applications necessitate the development of a robust and efficient airborne computing platform capable of delivering the required computing capability and efficiency, which are critical for the successful operation of UAVs.

Clearly, the design of such a UAV-based airborne computing platform presents several challenges. Physical constraints of UAVs, such as weight, size, power supply, and payload capacity, can limit the choice of suitable computing platform hardware, potentially impacting the overall performance of the platform and the applications it supports. For instance, due to UAV payload limitations, the computing platform must be lightweight and compact, while also being power-efficient to enable extended operation periods without recharging. These challenges and constraints were thoroughly analyzed in our previous studies [1], [2].

To address these challenges, our team developed a UAV-based airborne computing platform leveraging NVIDIA's Jetson TX2 [1], [2], [3], [4]. This high-performance, energy-efficient embedded platform, equipped with powerful graphic processing units (GPUs) and multiple central processing units (CPUs), enables swift processing of complex algorithms. The Jetson TX2 platform was selected due to its ability to meet the physical constraints of UAVs while providing the necessary computational power for various applications. Further details of this platform and more of our previous studies can be found in [5].

Despite the advantages of our current platform, it has certain limitations that need to be addressed. A significant limitation is

TABLE I
COMPARISON OF EXISTING STUDIES

| Ref. | Open computing platform | Algorithm for specific topics | Simulation | Implementation | Performance Evaluation | Year |
|---|---|---|---|---|---|---|
| [8] | ✓ | | | ✓ | | 2023 |
| [9] | ✓ | | | ✓ | ✓ | 2020 |
| [10] | | ✓ | ✓ | | | 2017 |
| [11] | | ✓(NOMA) | ✓ | | ✓ | 2017 |
| [12] | | ✓ | ✓ | | ✓ | 2019 |
| [13] | | ✓ | ✓ | | ✓ | 2023 |
| [14] | | ✓ | ✓ | | ✓ | 2023 |
| Ours | ✓ | | | ✓ | ✓ | 2024 |

that our current platform only supports Wi-Fi connectivity and lacks support for cellular connectivity. Over the past decade, cellular systems have become increasingly important, with research focusing on the design, development, and deployment of generations of cellular systems, from the fourth generation (4G) to the future sixth generation (6G) systems. Cellular connectivity is expected to become a crucial component of many existing and future UAV applications. This important trend underscores the need for further development and adaptation of our UAV platform to fully support these crucial communication capabilities.

Enabling cellular connectivity in a UAV platform can be approached in two ways: integrating a user equipment (UE) device into the UAV or incorporating a cellular base station into the UAV-based airborne computing platform. While the former is a straightforward solution, it is the latter, a more challenging approach that we focus on in this paper. The integration of a cellular base station into a UAV platform offers several advantages over simply adding a UE device. Firstly, it allows the UAV to serve as a mobile base station, extending network coverage to areas that may be underserved or completely lack for cellular connectivity. Secondly, it enables the UAV to directly manage and control wireless communication, providing greater flexibility and adaptability in dynamic environments. Lastly, it opens up the possibility for the UAV to serve multiple ground devices simultaneously, thereby fully leveraging the computing capabilities of our airborne computing platform.

In the literature, there have been a few recent studies that present UAV-based base stations, such as the use of tethered drones as aerial base stations in cellular networks to enhance coverage and capacity [6]. However, these existing approaches typically rely on commercial base stations and cannot be directly applied to our platform. Recognizing the critical role of Long-Term Evolution (LTE) in providing robust and reliable wireless communication, as well as its compatibility with current and future cellular systems, we aim to develop a UAV-integrated LTE base station using software-defined radio (SDR) technology. SDR offers programmability and flexibility, making it an ideal solution for our platform. By integrating an LTE base station into our UAV platform, we can leverage the widespread adoption and advanced capabilities of LTE to provide enhanced connectivity for UAV applications. In [7] the authors also propose a flying UAV prototype and show the hardware components, but the system is different to our work in the following ways: 1) since [7] uses a commercial UAV, it does not show what computing platform is used and how the computing platform impacts the system implementation and communication performance; 2) while integrating with SDR, the system in [7] may require addressing compatible hardware and software, which is not illustrated in this paper, and 3) the Evolved NodeB (eNB) is on UAV but the core network is still on the ground. Table I compares other related work in literature.

Fundamentally, the design of an SDR-based system is rooted in the concept of utilizing software to process signals in radio technology, as opposed to relying solely on hardware-based methods [14]. This approach has led to the development of numerous SDR-based prototypes in recent years, spanning various wireless technologies such as Bluetooth [15], Wi-Fi [16], [17], satellite communications [18], etc. While there have been developments in SDR-based cellular base stations, most existing prototypes employ regular computers with general-purpose processors (GPPs) as the computing platform [19]. Clearly, these solutions may not be suitable for UAVs due to the size and power constraints. To the best of our knowledge, there is a lack of UAV platforms that support SDR-based cellular base stations, and the performance analysis of such a system remains largely uncharted territory.

In this paper, we present an enhanced version of our UAV-based airborne computing platform that integrates SDR technology to facilitate cellular connectivity. Specifically, we identify and implement a suitable SDR module and open-source software to transform our platform into an LTE base station. This transformation not only provides robust computing power but also enables seamless communication between the UAV and a multitude of LTE-enabled ground devices. By leveraging the widespread adoption and advanced capabilities of LTE, we significantly broaden the potential applications of our platform, opening up new possibilities for UAV applications in various fields.

The primary contributions of this paper are as follows:

1) We provide a comprehensive description of the design and implementation of two types of SDR-enabled LTE base stations: one using a laptop computer with GPPs and the other using our UAV platform. We explore both the hardware and software components of our prototypes, emphasizing the integration of SDR technology within the constraints of UAVs. This includes the selection of the SDR module, the configuration of the software, and

the process of integrating these components into our UAV platform.

2) Utilizing the prototypes we develop, we conduct extensive experiments to evaluate the performance of our new systems in both indoor and outdoor scenarios. These experiments focus on a variety of performance metrics, including latency, throughput, signal-to-noise ratio (SNR), and resource consumption. Our results reveal the impact of the computing platform on system performance, with the UAV-based system exhibiting higher latency and lower throughput compared to the laptop-based system. However, we also observe a larger SNR variation in the UAV-based system, suggesting potential performance improvements with software optimization.
3) By comparing the performance of the two types of LTE base stations, we identify critical issues and provide insights into the impact of the computing platform, the importance of software and hardware separation, and the potential for software optimization. These findings can inform and facilitate the development of future UAV-based airborne computing platforms with SDR capability. Ultimately, our work enhances the performance and capabilities of UAV-based airborne computing platforms, paving the way for supporting a wide range of potential UAV applications.

The rest of this paper is organized as follows. In Section II, we first discuss the background of cellular systems, from 4G (LTE) to future 6G. In Section III, we detail our system design, discussing the selection of computing platforms, SDR hardware, software setup, and the integration of UE into our LTE system. We then discuss the experimental setup and results in Section IV, before concluding the paper in Section V.

## II. The Background of Cellular Systems

In this section, we first discuss the standards of cellular systems specified by the International Telecommunication Union - Radiocommunication Sector (ITU-R). We then briefly summarize industrial standards specified by the Third Generation Partnership Project (3GPP). Finally, we introduce the main components of a standard LTE system.

### A. ITU-R Standards

For the standardization of cellular systems, ITU-R plays a crucial role in defining the requirements for each generation of mobile communication systems. Specifically, for the fourth generation (4G), the ITU-R defined the International Mobile Telecommunications Advanced (IMT-Advanced) standard in 2008 [20], which set the stage for high-speed mobile broadband and multimedia applications. For instance, the IMT-Advanced standard requires a 4G system to support up to 1 Gbps data rate for a client with low mobility and up to 100 Mbps data rate for a client with high mobility.

For the fifth generation (5G), the ITU-R developed the IMT-2020 standard in 2015 [21]. This standard aims to support the massive growth in connectivity and data traffic, with requirements for higher data rates (e.g., downlink peak data rate up to 20 Gbps), lower latency (e.g., as low as 1 ms under the Ultra Reliable Low Latency Communications (URLLC) service), and greater device connectivity (e.g., supporting both typical mobile devices and IoT devices).

Looking forward, the ITU-R has begun the process of defining the requirements for the sixth generation (6G) under the IMT-2030 standard [22]. While the specific requirements are still under discussion, it is expected that 6G will further enhance the capabilities of 5G, with a focus on areas such as ubiquitous connectivity, integrated artificial intelligence (AI) and communications, and integrated sensing and communications.

### B. 3GPP Standards

To develop actual cellular systems that fulfill the ITU-R requirements, 3GPP is the organization that defines protocols and systems in different releases [23]. Specifically, 3GPP published the first LTE standard in 3GPP Release 8 in 2008, mainly about the radio interface. Then, in 2011, 3GPP published Release 10 that fulfills the IMT-Advanced standard, which is known as LTE-Advanced and is considered the first 4G standard defined by 3GPP. In the next few years, 3GPP continued to develop new standards to enhance the capability of LTE from Release 11 to Release 14, which was published in 2017.

For 5G systems, 3GPP published Release 15 in 2018 that defines 5G New Radio (5G NR). Since then, the latest 5G standard defined by 3GPP is Release 17 [24], which was published at the end of 2022. Currently, 3GPP is working on the next version of 5G, which is known as the 5G-Advanced, under Release 18.

### C. LTE

As introduced above, LTE is a wireless communication standard developed by the 3GPP [23]. As a cornerstone of 4G mobile communication, LTE has achieved significant commercial success, with billions of devices worldwide supporting this standard currently. This widespread adoption underscores the importance and relevance of LTE in today's wireless communication landscape. In addition to this justification, we also note that LTE supports a wide range of frequency bands and bandwidths, enabling high-speed data transmission and efficient use of the radio spectrum. The high-frequency transmission inherent in LTE necessitates high-rate sampling, real-time encoding/decoding, modulation/demodulation, and strict adherence to network delay specifications to maintain a continuous connection. Furthermore, the processing of LTE protocols, such as the Stream Control Transmission Protocol (SCTP), involves complex procedures for channel access, routing, handover, and managing end-to-end dialogues. These tasks require powerful computing capabilities to ensure efficient and reliable communication. Clearly, the computational demands of LTE signal processing and protocol processing can place significant force on a computing platform, particularly in terms of computing capability and efficiency. Therefore, the development of an LTE base station on a UAV platform represents a significant step toward enhancing the connectivity and versatility of UAV applications.

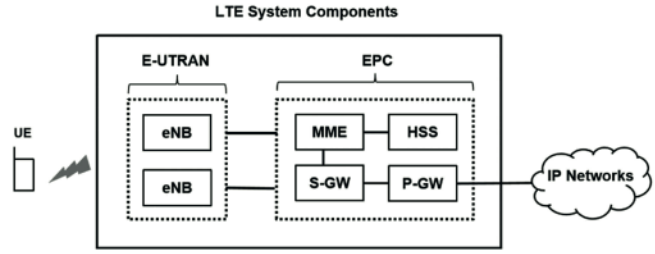


Fig. 1. An overview for LTE systems that shows main components related to this paper.

As shown in Fig. 1, an LTE system comprises several key components: User Equipment (UE), the Evolved Universal Terrestrial Radio Access Network (E-UTRAN), the Evolved Packet Core (EPC), and IP Networks. The EPC, which is composed of multiple logical nodes including the Mobility Management Entity (MME), Home Subscriber Server (HSS), Serving Gateway (S-GW), and Packet Data Network (PDN) Gateway (P-GW), plays a crucial role in authenticating subscribers and locating the UE. On the other hand, the E-UTRAN, consisting of multiple Evolved NodeBs (eNBs), manages radio access and sessions. These eNBs establish wireless connections with UEs, facilitating seamless communication within the network [23].

The widespread success of LTE, particularly in smartphone applications, has sparked considerable research interest in exploring LTE performance through SDR-based testbeds. For example, Gomez-Miguelez et al. introduce an open-source platform for LTE experimentation, which includes support for both LTE library (srsLTE) and UE (srsUE) in full compliance with LTE Release 8 [19]. In recent years, this open-source platform has been extended to accommodate new cellular systems, including 5G [25]. Other research efforts have developed SDR-based testbeds to validate performance metrics such as throughput in LTE and license-assisted access (LAA) coexistence systems [26]. These studies show the potential of SDR as a valuable tool for implementing and enhancing LTE systems, as well as 6G and NextG networks [27].

### D. NTN and Open RAN

NTN (Non-Terrestrial Networks) [28], [29] consists of communication networks that extend beyond traditional terrestrial infrastructure, incorporating various technologies and platforms such as satellites, UAVs, high-altitude platforms (HAPs), and maritime systems. Specifically, in the latest 3GPP Release 17, 5G architecture that utilizes satellite as infrastructure has been defined. However, the same release only considers UAV as UE. Therefore, our research on UAV-enabled base stations may facilitate much advanced research in the area of NTN.

The Open RAN [30] is a new paradigm for the next generations of radio access network (RAN) architecture. By deploying disaggregated, virtualized, and software-based components, Open RAN aims to support resiliency, reconfigurability, interoperability, and intelligence. In this paper, we develop an SDR-based platform, which shares the same key features with Open RAN, such as flexibility, cost-effectiveness, and interoperability within wireless communication networks. The platform we proposed aligns seamlessly with the principles of Open RAN and can be utilized to further develop Open RAN using our UAV platform. The implementation procedure and the lessons learned may facilitate better Open RAN design and deployment.

TABLE II
COMPUTING HARDWARE CHARACTERISTICS

| | Laptop | Jetson TX2 |
|---|---|---|
| **CPU** | Intel® Core™ i7-6700HQ CPU @ 2.60GHz × 8 | Dual-Core NVIDIA Denver 2 64-Bit CPU Quad-Core ARM® Cortex®-A57 MPCore |
| **GPU** | None | 256-core NVIDIA Pascal™ GPU architecture with 256 NVIDIA CUDA cores |
| **Memory** | 32GB | 8GB |
| **OS** | Ubuntu 18.04 LTS | Ubuntu 18.04 LTS |

## III. THE SYSTEM DESIGN

In this section, we discuss the design of a comprehensive LTE system, encompassing both the UE devices and the LTE base stations. We begin by discussing the computing devices essential for an SDR system. Following this, we detail the process of selecting the SDR hardware to be integrated into our UAV-based airborne computing platform. Subsequently, we elaborate on the LTE software system that underpins our design. Finally, we provide a brief explanation of the UE devices incorporated into our LTE system.

### A. The Computing Platforms

In this study, we employ two distinct computing platforms to implement and evaluate our LTE system: 1) our UAV-based airborne computing platform powered by NVIDIA's Jetson TX2 that integrates CPU and GPU, and 2) a Dell Laptop equipped with Intel CPUs, a typical example of GPP. The Jetson TX2, serving as the computing unit in our UAV platform, has demonstrated its effectiveness in our previous studies [31]. For comparative analysis, we also assess an LTE system running on the Dell Laptop. The specifications of these two computing platforms are summarized in Table II.

The Jetson TX2, developed by NVIDIA, is a high-performance computing platform that leverages the NVIDIA Pascal architecture [31]. This compact yet powerful platform offers several advantages over traditional desktop PCs and laptops, particularly in terms of size, energy consumption, and computational capability. Its compact form factor allows it to be easily integrated into a UAV environment, while its powerful 64-bit ARM processors and NVIDIA Pascal GPU enable it to handle complex tasks, such as wireless communication protocols and video processing, that would typically pose a challenge for other compact platforms.

In addition to its hardware capabilities, the Jetson TX2 also benefits from the integration of multiple software libraries, including Jetpack, CUDA, TensorRT, and high-performance

TABLE III
COMPARSION OF SDR PLATFORMS

| | USRP B210 | LimeSDR Mini | LimeSDR USB |
|---|---|---|---|
| **Frequency** | 70 MHz – 6 GHz | 100 kHz – 3.8 GHz | 100 kHz – 3.8 GHz |
| **Bandwidth** | 56 MHz | 30.72 MHz | 61.44 MHz |
| **Cost** | $1,472.00 | $186.95 | $349.95 |
| **Weight** | 350 g | 20 g | 118 g |
| **Dimension** | 97mm x 15.5mm | 69mm x 31.4mm | 100mm x 60mm |
| **Power** | USB 3.0, DC 6V | USB 3.0, DC 6V | USB 3.0, DC 6V |

computing (HPC) [32]. These libraries facilitate a range of functionalities, such as deep learning, multimedia processing, and GPU computing, thereby enhancing the platform's overall computational intelligence.

Despite its robust processing power, the Jetson TX2 maintains a low energy footprint, consuming around 7.5 watts of power. This is significantly less than the power consumption of traditional GPPs and older NVIDIA Jetson modules. The combination of high processing efficiency and low power consumption makes the Jetson TX2 an ideal choice for UAVs, where power conservation is critical for extending flight time.

It is worth noting that since the development of our airborne computing platform, NVIDIA has introduced two new generations of processing units: Xavier and Orin. These processors offer enhanced performance and efficiency compared to the Jetson TX2, potentially providing even greater computational capabilities for our LTE system. Importantly, our platform's design is flexible and adaptable, allowing it to be readily ported to these newer NVIDIA processors. This adaptability ensures that our platform remains up-to-date with the latest advancements in processing technology, thereby enhancing its potential for supporting advanced UAV applications.

### B. The SDR Hardware

Software-defined radio (SDR) technology provides a flexible and cost-effective solution for prototyping wireless communication systems, as it allows radio spectrum operations to be performed by customized software rather than specialized hardware [14]. An SDR platform typically consists of a programmable RF front-end and application-oriented software. This technology offers numerous benefits, including flexibility, cost-effectiveness, easy replication, and reduced life cycle. For instance, an SDR platform can support various standards like FM/AM radio, Wi-Fi, Bluetooth, and LTE, allowing for the reuse of software modules for different frequency and modulation techniques according to design requirements [33], [34].

In our design, we aim to develop a compact SDR system that can be deployed on autonomous systems like UAVs, which may function as edge computing nodes. To this end, we select the LimeSDR USB as our SDR hardware platform. As shown in Table III, the LimeSDR USB provides a good trade-off between performance and physical parameters. It is compact in size (100 mm $\times$ 60 mm with a weight of 118 grams), making it suitable for integration into a UAV. Moreover, the LimeSDR USB is equipped with an Altera Cyclone IV FPGA, which provides high computing power. It covers a frequency range between 100 kHz and 3.8 GHz with a bandwidth of 61.44 MHz, which satisfies the requirements of most wireless communications.

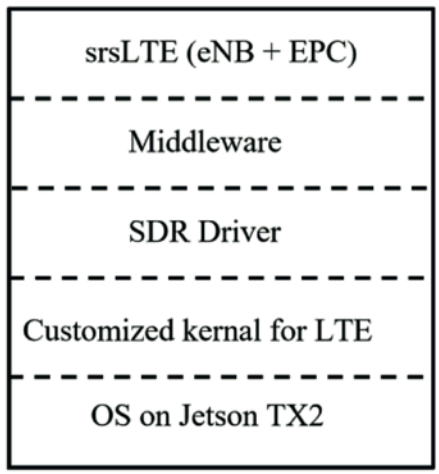


Fig. 2. An overview for LTE system software.

It is worth noting that the selection of SDR hardware is a critical step in the design of an SDR-based LTE system. The chosen hardware must not only meet the technical requirements of the system but also be compatible with the physical constraints of the deployment environment. In the case of UAV-based systems, factors such as size, weight, and power consumption are particularly important. The LimeSDR USB, with its compact size, lightweight design, and efficient power consumption, is well-suited to this application.

### C. The LTE System Software

In our design, we aim to incorporate the functionalities of both E-UTRAN and EPC into our UAV-based airborne computing platform. To enable this integration, our software stack comprises the Jetson TX2 system kernel, LimeSuite (version 20.01) as the SDR driver, SoapySDR (version 0.7.1), and srsLTE (version release 19.12). These components of our software stack are illustrated in Fig. 2.

*1) System Kernel:* During our investigation, we find that the Stream Control Transmission Protocol (SCTP), a protocol integral to the communication between eNB and EPC, is disabled in the default Jetson TX2 kernel. To address this, we compile a custom kernel from the source code downloaded from the official NVIDIA website [32]. In the process of generating a Linux kernel for enabling SCTP on Jetson TX2, we modify the

configuration files to define a local version for the kernel, which serves as an identifier for all its modules, and to activate the SCTP option. After these modifications, we renew the kernel file in the boot directory. Upon rebooting the system, the new kernel, now equipped with LTE capacity, is available for use.

*2) SDR Driver:* Given our use of the LimeSDR USB board as the RF front-end for our LTE system, we need to install the corresponding driver, LimeSuite (version 20.01). We accomplish this by locally compiling the driver from its source code [35].

*3) Middleware:* To facilitate the operation of our LTE system, we install SoapySDR (version 0.7.1), a middleware solution. SoapySDR serves as a wrapper, translating lower-level interfaces from the C language to the Python language and encapsulating them into APIs. This abstraction allows upper-level software to configure and monitor the SDR device, irrespective of the environment in which it operates or the interfaces it uses. We install SoapySDR by locally compiling it from the source code [36].

*4) Software for eNB and EPC:* For our eNB and EPC software, we choose the srsLTE project (now known as srsRAN) after evaluating ongoing open-source LTE platform options, such as srsLTE [25] and OpenAirInterface (OAI) [37]. The srsLTE/srsRAN is a lightweight project, easily deployed and providing all the LTE components, i.e., UE, eNB, and EPC. Besides supporting the flexible network prototype, the srsLTE/srsRAN project has been releasing new versions to comply with the network standard evolution. Therefore, the srsLTE/srsRAN is an ideal fit for our study. For our system, we install srsLTE (version release 19.12[1]) by locally compiling it from the source code [38]. The design of the srsLTE/srsRAN project allows the eNB and EPC to run on either a single machine or two separate machines. In our implementation, we run both components on a single machine.

### D. The UE in Our System

In our LTE system, we mainly utilize a commercial off-the-shelf (COTS) mobile device, specifically, Apple iPhone 7 Standard Edition, as the User Equipment (UE) shown in Fig. 1. To facilitate network access, we insert a programmable SIM card from the Open Cells project [39] into the UE. This SIM card can be configured with the necessary International Mobile Subscriber Identity (IMSI) and authentication information. Consequently, our UE is capable of establishing a connection with the eNB and EPC that we have implemented on our UAV-based airborne computing platform. Additionally, to identify the LTE signals from our UAV-based airborne computing platform, we use another COTS mobile device, Samsung Galaxy S9+, to observe and present the network parameters.

## IV. Experimental Setup and Results

In this section, we first provide a detailed description of our experimental setup, including the configuration of all system components. Next, we present the performance of our LTE system in both indoor and outdoor scenarios. Finally, we discuss the key insights we have gained from these results.

[1]This version of srsLTE/srsRAN also supports 5G NR, although we only utilize its LTE capabilities in our implementation.

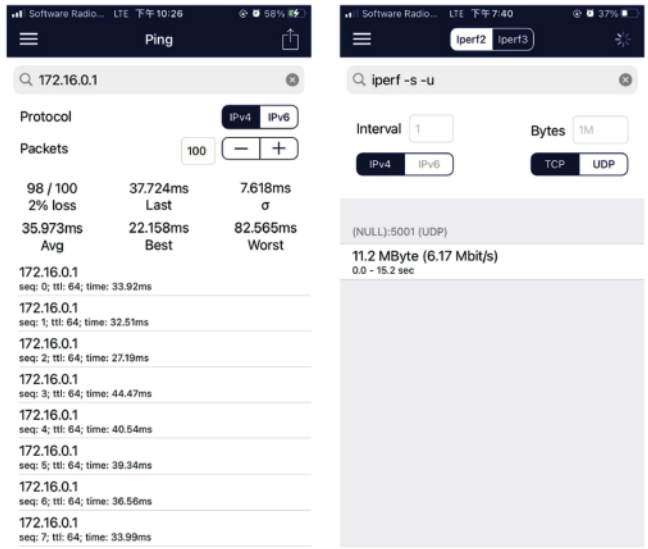


Fig. 3. System performance parameters tested and shown on UE (COTS mobile device: iPhone 7, App: Network Tools). (a) Screenshot of testing delay (b) Screenshot of testing throughput.

### A. Experimental Setup

We conduct our experiments in two different settings: an indoor lab environment with a stationary UAV and an outdoor environment with the UAV in flight. The frequency and bandwidth configuration, SDR setup, and testing environments are kept consistent across both settings. Next, we will explain the details of our experiments.

*1) Frequency and Bandwidth:* To avoid interference with local LTE services, we select Band 3 for the radio frequency. We implement frequency division duplexing (FDD), setting the uplink carrier frequency to 1787.4 MHz and the downlink carrier frequency to 1878.4 MHz. A bandwidth of 3 MHz is chosen for our cellular network.

*2) SDR Configuration:* Our LimeSDR setup supports both single and multiple antennas. As an initial phase of our research, we utilize a single antenna configuration on the LimeSDR. Specifically, the RX1-L port on the SDR board is used for the receive channel, and the TX1-1 port for the transmission channel.

*3) UE Configuration:* In our experiments, we mainly utilize the iPhone 7 as the test tool to connect our SDR-enabled LTE base station. To test the system performance through UE, we send commands by using an App named Network Tools and get the system performance metrics on the App. As shown in Fig. 3, we send the ping command and the iperf command to obtain the latency and throughput performance, respectively. The displayed details show the base station gateway that we set up (172.16.0.1 on the command line in Fig. 3(a) and (b)) and the performance metrics, such as delay and throughput parameters. Specifically, in this example, Fig. 3(a) shows that the

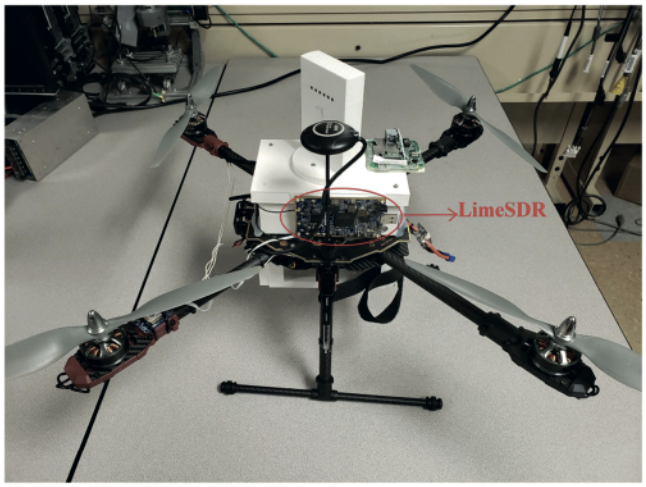


Fig. 4. Our UAV-based airborne computing platform in the indoor scenario.

Fig. 5. Our UAV-based airborne computing platform in the outdoor scenario.

average delay is 35.973 ms and the standard deviation (SD) of the delay is 7.618 ms, while Fig. 3(b) shows that the throughput is 6.17 Mbps.

*4) Testing Environments:* To evaluate the performance of our SDR-based LTE base station that is integrated into the UAV-based airborne computing platform, we conduct experiments in practical settings that aim to emulate a realistic LTE network environment. Our testing environments encompass both controlled indoor scenarios (shown in Fig. 4) and dynamic outdoor conditions (shown in Fig. 5).

In the controlled indoor setting, we vary the distances between the user equipment (UE) device and the eNB (base station) to analyze performance metrics relative to distance. The testing environment is a rectangular room with a length of approximately 5 meters. During the testing process, the Jetson TX2 (eNB) was placed at one end of the room, and the UE was moved to distances ranging from 0.5 meters to 5 meters away from the Jetson TX2. This allows us to assess the impact of signal strength, data rates, and other performance indicators as the UE device moves further away from the base station. Additionally, we monitor the real-time utilization of computing resources on both the UAV-based system and the laptop-based system to evaluate the impact of the computing platforms on software performance.

In the second experimental setting, we specifically focus on evaluating the performance of the LTE system when deploying it on the drone in an outdoor environment. This setup enables us to investigate the feasibility and effectiveness of a mobile LTE system in real-world conditions. Notably, we migrate the LTE system onto the drone without modifying any system modules or configurations, ensuring consistency with the ground-based setup. To remotely monitor the LTE system, we utilize the Wi-Fi connection from a test laptop to the LTE system on the drone. This allows us to send commands and inspect the results while the drone is in flight.

Due to the drone's mobility and the vast distances it can cover in outdoor environments, we conduct our tests with a larger distance interval compared to indoor scenarios. This approach facilitates the observation of noticeable performance differences and provides insights into the system's behavior under challenging conditions and varying signal strengths. Specifically, we select two points where the UE is positioned at a considerable distance from the LTE system, specifically at 3 meters and 5 meters. These distances are chosen to examine the system's performance and capabilities in scenarios involving greater physical separation between the UE and the LTE base station.

*5) System Parameters Observed by UE:* After setting up the system, we can observe the system parameters from the UE side. As shown in Fig. 6, the screenshots taken on the Samsung phone confirm the presence of established signals and provide key information about the LTE system. The displayed details include the utilization of Band 3, Downlink (DL) frequency, and Uplink (UL) frequency (represented by the E-UTRA Absolute Radio Frequency Channel Number (EARFCN) component in Fig. 6), as well as the information of the software, i.e., srsLTE (indicated by the carrier information in Fig. 6).

Furthermore, through signal detection, we can find the power of the received signal. Specifically, Fig. 6 shows that, at distances of 3 meters and 5 meters, the power of received signals are $-93.0\,dBm$ (4 bars) and $-101.0$ dBm (3 bars), respectively, in two experiments.

### B. Results in the Indoor Scenario

*1) End-to-End Delay:* We start our investigation by evaluating the end-to-end delay, a critical performance metric in wireless communication systems that is regularly measured by practitioners, researchers, and vendors. In our experimental setup, when the UE is powered on or transitions from airplane


Fig. 6. System parameters detected by UE (App: LTE Discovery). (a) Screenshot at 3 meters. (b) Screenshot at 5 meters.

mode to the wireless environment, it initiates a search for wireless signals. Once the UE attaches to the network established by our prototype, it acquires an IP address (either IPv4 or IPv6). For our system, we configure the EPC to operate at the IPv4 mode, setting up an IPv4 gateway and allocating IPv4 addresses to the UEs.

To measure latency as a function of distance, we execute the ping command separately on the UE and the EPC to obtain the Round Trip Time (RTT) when the connection is established. We send packets at one-second intervals for a total of 100 seconds at each location. This experiment is repeated six times at each location, and the average RTT and 95% confidence interval are used as the experimental data in Fig. 7. The measurements are conducted at different locations with distances ranging from 0.5 meters to 5 meters.

Since we implement two LTE systems, one utilizing our airborne computing platform and the other employing a laptop computer, we compare the performance measured at eNB in Fig. 7(a), and the performance measured at UE in Fig. 7(b). Both figures demonstrate that the latency is rather stable with a small range for confidence interval when the distance increases from 0.5 meters to 4.5 meters. On the other hand, when the distance increases from 4.5 meters to 5.0 meters, the RTT increases quite significantly with large confidence intervals, which could be due to the indoor environment of our experiments. Furthermore, the results indicate that the LTE system utilizing the Jetson TX2 exhibits slightly higher latency compared to the LTE system developed using the laptop.

*2) Throughput:* Next, we investigate the throughput performance of the cellular network by evaluating the transmission of User Datagram Protocol (UDP) packets between the UE and the EPC. To generate the UDP packets and assess the downlink performance, we utilize the iPerf tool, where the UE operates as

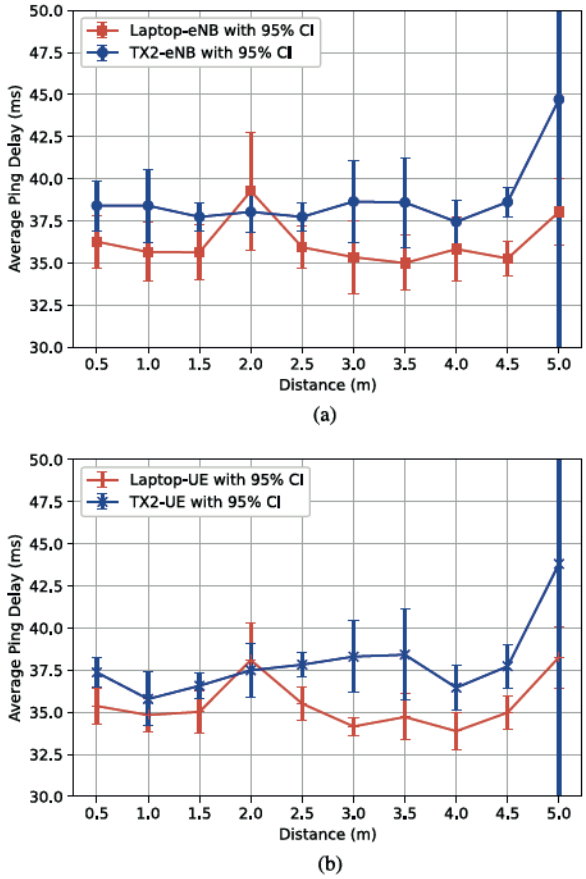


Fig. 7. RTT versus the distances between UE and eNB-EPC. (a) Average RTT at eNB. (b) Average RTT at UE.

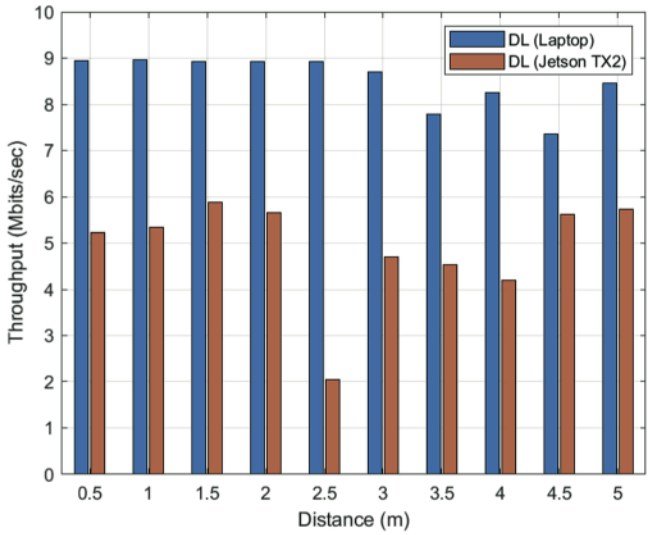


Fig. 8. The throughput versus the distances between UE and eNB-EPC.

the server and the EPC operates as the client. In our experiments, we measure the average transmission rate by sending a specified amount of UDP packets every second for a duration of 15 seconds. The throughput performance is then determined by averaging the results from three tests conducted at each location.

Fig. 8 presents the downlink throughput performance comparison between the two systems. This figure clearly illustrates

that the LTE system utilizing the Jetson TX2 achieves a lower throughput, approximately two-thirds of the throughput attained by the LTE system utilizing the laptop PC. We will discuss possible reasons at the end of this section. Additionally, a notable observation from the figure is that as the distance increases from 0.5 meters to 5 meters, the throughput experiences only a marginal decrease in both systems. This is significant because the LTE system has no power amplifier for the RF transceivers.

From Fig. 8, we notice a significant throughput drop at 2.5 m on the Jetson TX2 platform. As we know, various factors in the indoor environment, including spatial layout, walls, furniture, and even wall materials, can affect signal strength and impact throughput. When the UE was positioned at the midpoint of the room, approximately 2.5 meters away from the Jetson TX2, the influence of the walls was at an intermediate level. Our testing data indeed confirms that the throughput was lowest at this point, aligning with the expected trend of environmental effects on signal strength and throughput.

*3) Signal-to-Noise Ratio:* To measure the downlink Signal-to-Noise Ratio (SNR), we utilize the iPerf tool on the eNB to generate UDP packets. As these packets are transmitted from the eNB to the UE, we monitor uplink and downlink parameters, such as uplink SNR and uplink Power Headroom Report (PHR), using the eNB's monitoring capabilities. In an LTE network, the UE must adapt to the network's condition, report its status, and balance resource consumption for applications. The PHR serves as an indicator of the UE's available extra power for future transmission. To represent the SNR, we introduce an *equivalent SNR* parameter that combines the PHR with the SNR measurement. For the purposes of our discussion, the term SNR refers to this equivalent SNR. We obtain these parameters at one-second intervals using the srsLTE software and conduct the SNR inspection process over a duration of 15 seconds. For each given distance, we collect a large number of measurements and calculate the average SNR.

Fig. 9(a) presents the experimental results of SNR for the system based on the Jetson TX2. The SNR plots reveal small-scale fading at fixed distances and significant variation in the SNR for the LTE base station enabled by our airborne computing platform. Interestingly, the trend of average SNR does not show a substantial decrease with increasing distance, possibly due to the indoor environment's significant multipath effects. Fig. 9(a) also shows the linear regression for the relationship between SNR and the logarithm of the distance, indicating a slight decrease in SNR (less than 10 dB) as the distance increases from 0.5 meters to 5 meters. Fig. 9(b) presents similar results for the LTE system using the laptop as the computing platform. Here, we observe smaller SNR fluctuations at each location, indicating more stable SNR performance. The linear regression of SNR appears consistent across different locations. It's worth noting that the results in Fig. 9(a) and (b) can be influenced by various factors, including the LTE protocol, the UE's power resource allocation mechanism, and the algorithms used by srsLTE to generate and display the results.

*4) Resource Consumption:* Considering the advancements in semiconductor technologies, modern computing systems are typically equipped with multiple CPU cores. These systems

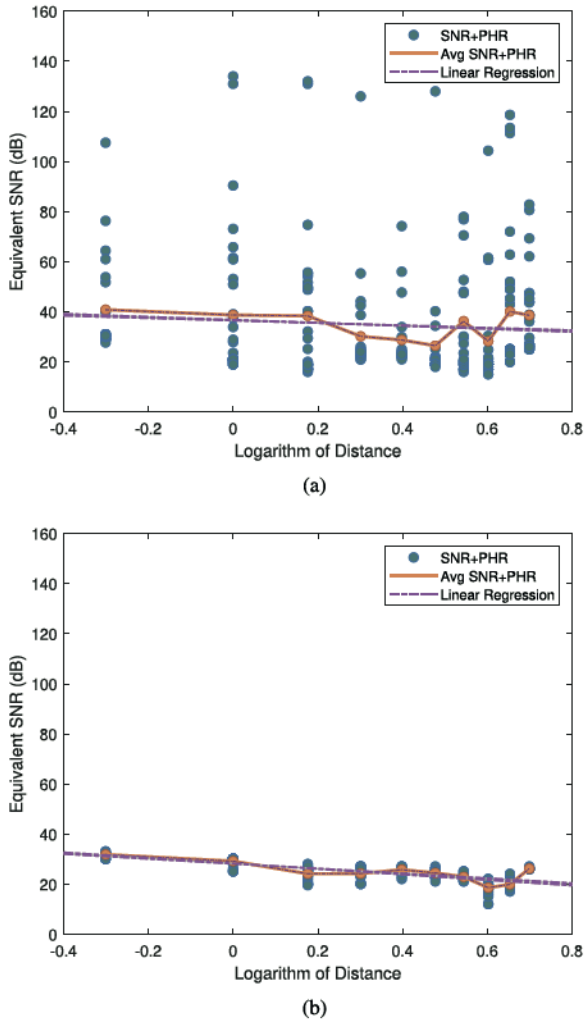


Fig. 9. Signal to Noise Ratio (SNR) versus distances (including SNR + PHR in each experiment, the average SNR + PHR vs. logarithm of distance, and the linear regression for SNR + PHR vs. logarithm of distance). (a) SNR over Jetson TX2 (b) SNR over Laptop.

employ default scheduling mechanisms to allocate computing tasks across the available cores. The objective of this experiment is to investigate the utilization of computing resources, specifically CPU and memory, and compare the performance between the LTE system with a laptop and the LTE system with the Jetson TX2 platform.

By default, we initiate the eNB and EPC programs on the Jetson TX2 using the respective commands, which dynamically assign processors for execution. We employ the `top` command to monitor the process state every second and collect data on CPU usage. The measurements are obtained over a period of ten minutes when no UE is attached to the network. It is important to note that the Jetson TX2 platform has six CPU cores, and each CPU may be allocated to execute threads of the eNB and EPC during the test duration. The operations of the eNB, EPC, and other system programs on this platform adhere to the system's default scheduling rules. To evaluate the impact of the number of CPU cores on our application, we use the `taskset` command to restrict the application to run on a specific CPU. Employing

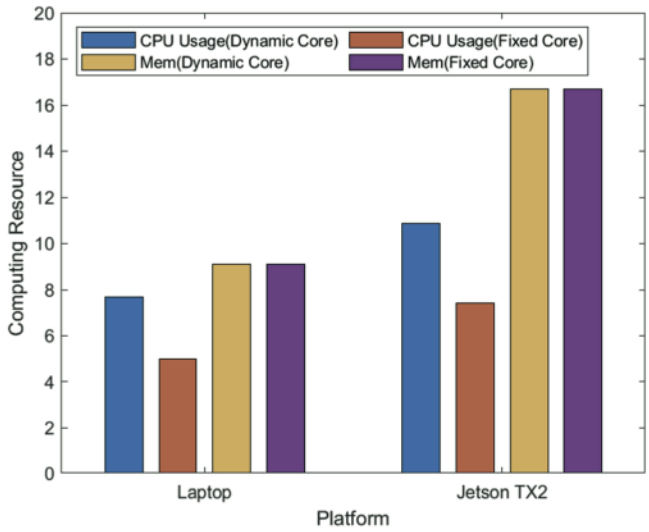


Fig. 10. Computing resources consumption on two computing platforms (Jetson TX2 and Laptop).

the same test duration and data acquisition method, we obtain a second set of average CPU and memory usage on the Jetson TX2. Similarly, we collect measurements using a laptop.

Fig. 10 presents a summary of the experimental results, where the y-axis represents the percentage of computing resource consumption, including CPU and memory. Specifically, this figure shows that the memory usage seems similar for fixed CPU scheduling and dynamic CPU scheduling in both platforms. On the other hand, this figure also demonstrates noticeable variations in CPU usage between fixed CPU scheduling and dynamic CPU scheduling, which holds true for both the Jetson TX2 and the laptop. Here, it is interesting to observe that the fixed CPU mode consumes fewer CPU resources compared to the dynamic mode, with about 35% reduction (from 7.69% to 5.00%) for the laptop and about 32% reduction (from 10.85% to 7.42%) for the Jetson TX2. This observation can be attributed to the additional computing resources required for scheduling and task dispatch when utilizing multiple CPU cores. It also suggests that the current implementation of srsLTE has not fully leveraged the multi-CPU resources, emphasizing the need for future development in this area.

### C. Results in the Outdoor Scenario

*1) End-to-End Delay:* In the outdoor scenarios, we investigate the system performance at two specific distances between the UE and the LTE system: 3 meters and 5 meters. To ensure reliable and robust results, we conduct the experiments three times at each distance and average the experimental data. As shown in Table IV, the delay results of both scenarios are similar in most cases.

*2) Throughput:* The process of measuring experimental throughput follows a similar approach to that of measuring end-to-end delay. At the specified points, namely, from 3 meters to 12 meters, we conduct the iperf experiments for a duration of ten seconds. The experimental throughput results are presented

TABLE IV
THE AVERAGE AND SD OF RTT OF THE UAV-BASED COMPUTING PLATFORM IN INDOOR AND OUTDOOR SCENARIOS

| | | Average of RTT (ms) | | SD of RTT (ms) | |
|---|---|---|---|---|---|
| | | eNB Side | UE Side | eNB Side | UE Side |
| **3 meters** | **Indoor** | 38.649 | 38.3085 | 13.333 | 10.709 |
| | **Outdoor** | 35.808 | 31.267 | 6.566 | 11.883 |
| **5 meters** | **Indoor** | 44.713 | 43.812 | 14.714 | 14.715 |
| | **Outdoor** | 65.324 | 30.930 | 79.267 | 7.733 |

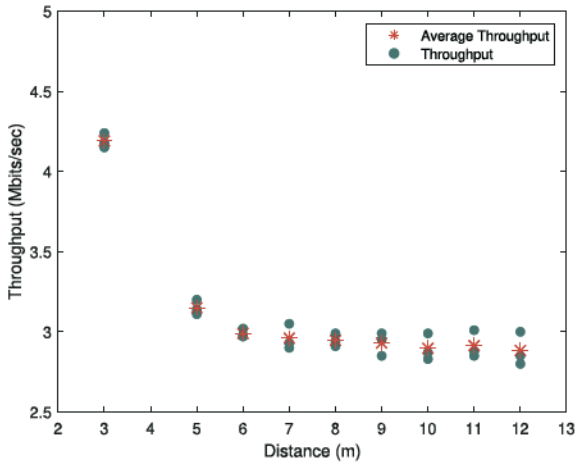


Fig. 11. Experiments over UAV: downlink throughput at 3–12 meters.

TABLE V
THE COMPARATIVE DOWNLINK THROUGHPUT OF THE UAV-BASED COMPUTING PLATFORM BETWEEN INDOOR AND OUTDOOR

| | Indoor | Outdoor |
|---|---|---|
| **3 meters** | 4.71 Mbps | 4.19 Mbps |
| **5 meters** | 5.73 Mbps | 3.15 Mbps |

in Fig. 11, which show that the throughput decreases significantly when the distance increases from 3 meters to 5 meters. On the other hand, the throughput decreases slightly when the distance increases from 5 meters to 12 meters. The comparison of throughput between indoor and outdoor scenarios at 3 meters and 5 meters is shown in Table V.

*3) Signal-to-Noise Ratio:* We also calculate the equivalent SNR by combining the SNR and PHR in the system output. The experiments are repeated twice at each location, with each experiment spanning a duration of ten seconds. The results of these experiments, reflecting the equivalent SNR, are presented in Fig. 12. This figure shows that the equivalent SNR decreases significantly when the distance increases from 3 meters to 7 meters, and it decreases slightly beyond 7 meters. The comparison of equivalent SNR between indoor and outdoor scenarios at 3 meters and 5 meters is shown in Table VI.

### D. Discussions

In this study, we have successfully developed and tested a prototype of an LTE base station integrated into a UAV-based airborne computing platform. Our experimental setup allows

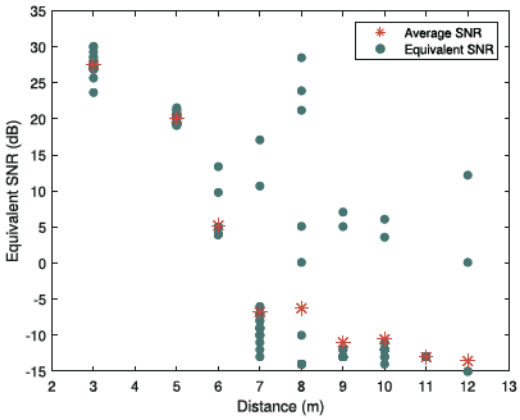


Fig. 12. Experiments over UAV: Equivalent SNR (SNR + PHR) at 3-12 meters.

TABLE VI
THE COMPARATIVE EQUIVALENT SNR (SNR + PHR) OF THE UAV-BASED COMPUTING PLATFORM BETWEEN INDOOR AND OUTDOOR

| | Indoor | Outdoor |
|---|---|---|
| **3 meters** | 26.448 dB | 27.456 dB |
| **5 meters** | 38.562 dB | 20.061 dB |

us to evaluate the system's performance in both indoor and outdoor scenarios, providing valuable insights into the practical implementation of such a system.

Our results clearly demonstrate the impact of the computing platform on the system's performance. Specifically, when compared to an LTE base station enabled by a laptop, the LTE base station built on our airborne computing platform exhibited a larger average and SD for RTT and lower throughput (approximately two-thirds of the laptop-based system). These results can be attributed to the smaller average SNR observed in the UAV-based system.

Interestingly, we also observed a larger variation in SNR for the UAV-based system, with some measurements nearing 140 dB. This suggests that the performance of the UAV-based system could be significantly enhanced through software optimization.

A crucial aspect of our system is the separation of software components from hardware components, which is also a key design principle in 5 G/6 G systems. Despite the advantages of such a design principle, our experiments also highlight the need for careful optimization to maximize system performance. For instance, our results show that, by simply fixing the CPU core assignment, we can decrease the CPU consumption by more than 30%. This finding underscores the importance of resource management techniques in the design and deployment of software applications on different computing platforms, particularly for complex systems like UAV-enabled LTE networks.

## V. CONCLUSION

In this paper, we have systematically investigated the development of an enhanced UAV-based airborne computing platform that integrates software-defined radio (SDR) technology to establish a Long-Term Evolution (LTE) base station. Such an enhanced platform can enable robust and reliable wireless communication and extend LTE network coverage to underserved areas. Specifically, we presented the detailed design and implementation process of our SDR-based LTE base station, including the selection of the computing platform, the SDR hardware, the LTE system software, and the User Equipment (UE). This comprehensive guide can serve as a valuable resource for similar future endeavors. Based on the detailed design, we have implemented prototypes and conducted extensive experiments to evaluate the performance of our system in both indoor and outdoor scenarios, focusing on key metrics such as latency, throughput, signal-to-noise ratio, and resource consumption. Notably, by comparing the performance of two types of LTE base stations, one utilizing a laptop computer and the other using our UAV platform, we observed that our UAV-based system demonstrated potential for substantial performance enhancement with software optimization. Our findings highlight the impact of the computing platform on system performance, emphasizing the feasibility of software and hardware separation and the potential for software optimization. Overall, our work contributes to the development of UAV-based airborne computing platforms with SDR capability, enhancing their communication capabilities and broadening their application potential. As LTE is compatible with current and future cellular systems, our research opens up new possibilities for UAV applications, such as edge computing, real-time object detection, remote sensing, and disaster management, all facilitated by the robust and reliable LTE connectivity provided by our UAV-based LTE base station.

## REFERENCES

[1] K. Lu, J. Xie, Y. Wan, and S. Fu, "Toward UAV-based airborne computing," *IEEE Wireless Commun.*, vol. 26, no. 6, pp. 172–179, Dec. 2019.
[2] B. Wang et al., "Computing in the air: An open airborne computing platform," *IET Commun.*, vol. 14, no. 15, pp. 2410–2419, 2020.
[3] B. Wang, J. Xie, S. Li, Y. Wan, S. Fu, and K. Lu, "Enabling high-performance onboard computing with virtualization for unmanned aerial systems," in *Proc. IEEE Int. Conf. Unmanned Aircr. Syst.*, 2018, pp. 202–211.
[4] S. Li et al., "Design and implementation of aerial communication using directional antennas: Learning control in unknown communication environments," *IET Control Theory Appl.*, vol. 13, no. 17, pp. 2906–2916, 2019.
[5] Airborne computing networks. Accessed: Jun. 25, 2024. [Online]. Available: https://utari.uta.edu/research/airborne/
[6] M. Kishk, A. Bader, and M.-S. Alouini, "Aerial base station deployment in 6G cellular networks using tethered drones: The mobility and endurance tradeoff," *IEEE Veh. Technol. Mag.*, vol. 15, no. 4, pp. 103–111, Dec. 2020.
[7] S.-Y. Chang, K. Park, J. Kim, and J. Kim, "Securing UAV flying base station for mobile networking: A review," *Future Internet*, vol. 15, no. 5, 2023, Art. no. 176.
[8] U. Fattore, M. Liebsch, and C. J. Bernardos, "UPFlight: An enabler for avionic MEC in a drone-extended 5G mobile network," in *Proc. IEEE 91st Veh. Technol. Conf.*, 2020, pp. 1–7.
[9] M. Mozaffari, W. Saad, M. Bennis, and M. Debbah, "Mobile unmanned aerial vehicles (UAVs) for energy-efficient Internet of Things communications," *IEEE Trans. Wireless Commun.*, vol. 16, no. 11, pp. 7574–7589, Nov. 2017.
[10] M. Nikooroo and Z. Becvar, "Optimal positioning of flying base stations and transmission power allocation in NOMA networks," *IEEE Trans. Wireless Commun.*, vol. 21, no. 2, pp. 1319–1334, Feb. 2022.
[11] J. Plachy, Z. Becvar, P. Mach, R. Marik, and M. Vondra, "Joint positioning of flying base stations and association of users: Evolutionary-based approach," *IEEE Access*, vol. 7, pp. 11454–11463, 2019.

[12] J. Zheng, Z. Wang, and A. Jamalipour, "An aerial and ground base station cooperation strategy for UAV and cellular integrated networks," *IEEE Internet Things J.*, vol. 11, no. 6, pp. 10411–10424, Mar. 2024.

[13] J. Zheng, Q. Zhu, and A. Jamalipour, "Content delivery performance analysis of a cache-enabled UAV base station assisted cellular network for metaverse users," *IEEE J. Sel. Areas Commun.*, vol. 42, no. 3, pp. 643–657, Mar. 2024.

[14] A. F. Selva, A. L. Reis, K. G. Lenzi, L. G. Meloni, and S. E. Barbin, "Introduction to the software-defined radio approach," *IEEE Latin Amer. Trans.*, vol. 10, no. 1, pp. 1156–1161, Jan. 2012.

[15] M. Jiang and W. Gong, "Bidirectional bluetooth backscatter with edges," *IEEE Trans. Mobile Comput.*, vol. 23, no. 2, pp. 1601–1612, Feb. 2024.

[16] C. Uysal and T. Filik, "A new RF sensing framework for human detection through the wall," *IEEE Trans. Veh. Technol.*, vol. 72, no. 3, pp. 3600–3610, Mar. 2023.

[17] M. S. Amjad et al., "Towards an IEEE 802.11 compliant system for outdoor vehicular visible light communications," *IEEE Trans. Veh. Technol.*, vol. 70, no. 6, pp. 5749–5761, Jun. 2021.

[18] A. Abdelaziz, R. Burton, F. Barickman, J. Martin, J. Weston, and C. E. Koksal, "Enhanced authentication based on angle of signal arrivals," *IEEE Trans. Veh. Technol.*, vol. 68, no. 5, pp. 4602–4614, May 2019.

[19] I. Gomez-Miguelez, A. Garcia-Saavedra, P. D. Sutton, P. Serrano, C. Cano, and D. J. Leith, "srsLTE: An open-source platform for LTE evolution and experimentation," in *Proc. 10th ACM Int. Workshop Wireless Netw. Testbeds Exp. Eval. Characterization*, 2016, pp. 25–32.

[20] ITU-R, "IMT-advanced," Accessed: Jun. 25, 2024. [Online]. Available: https://www.itu.int/en/ITU-R/study-groups/rsg5/rwp5d/imt-adv/Pages/default.aspx

[21] ITU-R, "IMT-2020," Accessed: Jun. 25, 2024. [Online]. Available: https://www.itu.int/en/ITU-R/study-groups/rsg5/rwp5d/imt-2020/Pages/default.aspx

[22] ITU-R, "IMT-2030," Accessed: Jun. 25, 2024. [Online]. Available: https://www.itu.int/en/ITU-R/study-groups/rsg5/rwp5d/imt-2030/Pages/default.aspx

[23] 3GPP specifications. Accessed: Jun. 25, 2024. [Online]. Available: https://www.3gpp.org/specifications

[24] 3GPP release 17. Accessed: Jun. 25, 2024. [Online]. Available: https://www.3gpp.org/specifications-technologies/releases/release-17

[25] srsRAN project. Accessed: Jun. 25, 2024. [Online]. Available: https://www.srslte.com/

[26] Y. Ma, R. Jacobs, D. G. Kuester, J. Coder, and W. Young, "SDR-based experiments for LTE-LAA based coexistence systems with improved design," in *Proc. IEEE Glob. Commun. Conf.*, 2017, pp. 1–6.

[27] M. Maier and D. T. Hoang, *6G and Onward to Next G: The Road to the Multiverse*. Wiley-IEEE Press, Feb. 2023.

[28] Release 17 description; summary of Rel-17 work items. Accessed: Jun. 25, 2024. [Online]. Available: https://portal.3gpp.org/desktopmodules/Specifications/SpecificationDetails.aspx?specificationId=3937

[29] M. M. Azari et al., "Evolution of non-terrestrial networks from 5G to 6G: A survey," *IEEE Commun. Surv. Tuts.*, vol. 24, no. 4, pp. 2633–2672, Fourthquarter 2022.

[30] M. Polese, L. Bonati, S. D'oro, S. Basagni, and T. Melodia, "Understanding O-RAN: Architecture, interfaces, algorithms, security, and research challenges," *IEEE Commun. Surv. Tuts.*, vol. 25, no. 2, pp. 1376–1411, Secondquarter 2023.

[31] Jetson TX2. Accessed: Jun. 25, 2024. [Online]. Available: https://developer.nvidia.com/embedded/jetson-tx2

[32] Jetson Download Center. Accessed: Jun. 25, 2024. [Online]. Available: https://developer.nvidia.com/embedded/downloads

[33] T. Juhana and S. Girianto, "An SDR-based multistation FM broadcasting monitoring system," in *Proc. 11th Int. Conf. Telecommun. Syst. Serv. Appl.*, 2017, pp. 1–4.

[34] M. Moradi, K. Sundaresan, E. Chai, S. Rangarajan, and Z. M. Mao, "SkyCore: Moving core to the edge for untethered and reliable UAV-Based LTE networks," *Commun. ACM*, vol. 64, no. 1, pp. 116–124, 2018.

[35] LimeSuite repository. Accessed: Jun. 25, 2024. [Online]. Available: https://github.com/myriadrf/LimeSuite

[36] SoapySDR repository. Accessed: Jun. 25, 2024. [Online]. Available: https://github.com/pothosware/SoapySDR

[37] OpenAirInterface (OAI) project. Accessed: Jun. 25, 2024. [Online]. Available: https://openairinterface.org/

[38] srsLTE. Accessed: Jun. 25, 2024. [Online]. Available: https://github.com/srsLTE

[39] Open cells project. Accessed: Jun. 25, 2024. [Online]. Available: https://open-cells.com/index.php/sim-cards/


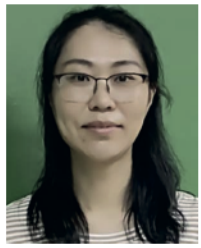

**Jinran Zhang** (Member, IEEE) received the B.S. and M.S. degrees in computer science and technology from the Beijing University of Posts and Telecommunications, Beijing, China. She is currently working toward the Ph.D. degree with the Department of Electrical Engineering, University of North Texas, Denton, TX, USA. Her research interests include unmanned aerial systems, computing platforms, collaborative networks, and system performance.

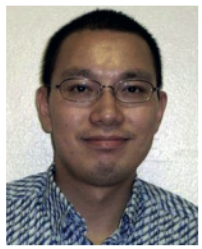

**Kejie Lu** (Senior Member, IEEE) received the B.Sc. and M.Sc. degrees from the Beijing University of Posts and Telecommunications, Beijing, China, in 1994 and 1997, respectively, and the Ph.D. degree in electrical engineering from the University of Texas at Dallas, Richardson, TX, USA, in 2003. In 2005, he joined the University of Puerto Rico at Mayagüez, Mayagüez, Puerto Rico, where he is currently a Professor with the Department of Computer Science and Engineering. His research interests include computer and communication networks, cyber-physical system, and network-based computing.

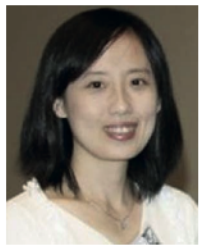

**Yan Wan** (Senior Member, IEEE) received the Ph.D. degree in electrical engineering from Washington State University, Pullman, WA, USA, in 2009. She did Postdoctoral training with the University of California, Santa Barbara, CA, USA. She is currently a Distinguished University Professor with Electrical Engineering Department, University of Texas at Arlington, Arlington, TX, USA. Her research interests include the modeling, evaluation, and control of large-scale dynamical networks, cyber-physical system, stochastic networks, decentralized control, learning control, networking, uncertainty analysis, algebraic graph theory, and their applications to unmanned aerial vehicle (UAV) networking, UAV traffic management, epidemic spread, complex information networks, and air traffic management. Her research has led to over 190 publications and successful technology transfer outcomes.

**Junfei Xie** (Senior Member, IEEE) received the B.S. degree in electrical engineering from the University of Electronic Science and Technology of China, Chengdu, China, in 2012, and the M.S. degree in electrical engineering and the Ph.D. degree in computer science and engineering from the University of North Texas, Denton, TX, USA, in 2013 and 2016, respectively. From 2016 to 2019, she was an Assistant Professor with the Department of Computing Sciences, Texas A&M University-Corpus Christi, Corpus Christi, TX, USA. She is currently an Associate Professor with the Department of Electrical and Computer Engineering, San Diego State University, San Diego, CA, USA. Her research interests include large-scale dynamic system design and control, airborne networks, airborne computing, and air traffic flow management. She was the recipient of the NSF CAREER Award.

**Shengli Fu** (Senior Member, IEEE) received the B.S. and M.S. degrees in telecommunication engineering from the Beijing University of Posts and Telecommunications, Beijing, China, in 1994 and 1997, respectively, the second M.S. degree in computer engineering from Wright State University, Dayton, OH, USA, in 2002, and the Ph.D. degree in electrical engineering from the University of Delaware, Newark, DE, USA, in 2005. He is currently a Professor and the Chair with the Department of Electrical Engineering, University of North Texas, Denton, TX, USA. His research interests include coding and information theory, wireless communications and sensor networks, and aerial networks.